Supporting Information

Simulations of equilibrium and non-equilibrium mechanisms and analysis using third-order correlation functions. A simple cyclic mechanism was used to simulate channels that alternate between bursting and non-bursting states (**Figure S2**). Detailed balance violations can be introduced by changing the relative values of rate constants. Rate constants were as follows (sec^{-1}): k_{b1}, k_{1b}, k_{b3}, k_{3b} = 1000, k_{12}, k_{23} = 10, k_{34}, k_{41} = 1, and k_{14}, k_{43}, k_{32}, k_{21} = 0.001 for an irreversible mechanism (**Figure S2a**) and k_{14}, k_{43} = 1 and k_{32}, k_{21} = 10 for a reversible mechanism (**Figure S1b**). In the non-equilibrium mechanism, excursions through the $O_1 \rightarrow C_2 \rightarrow O_3 \rightarrow C_4$ cycle will be exclusively clockwise. Third-order correlation functions ($G_2 - G_2^T$) of simulated records from non-equilibrium and equilibrium mechanisms are shown in **Figure S3a** and **Figure S3b**, respectively.

Higher-order correlation analysis can be used to test for microscopic reversibility in single-molecule systems.[1,2] In practice, however, this analysis requires that fluctuations in the signal are relatively large compared to the mean. When the number of channels and/or the open probability is sufficiently high, random variation in G_2 will be large proportional to the mean compared to $G_2 - G_2^T$. Thus, microscopic reversibility violations will not be detectable even if they are present.

To determine the lower limit of $(G_2 - G_2^T) / G_2$ for which violations of microscopic reversibility are still detectable, simulations of equilibrium and non-equilibrium mechanisms of ~100 sec (similar to experimental records) were carried out, and third-order correlation functions were determined for channel activity averaged over 100 ms. For $(G_2 - G_2^T) / G_2 \geq \sim 0.1$, the

reversible and irreversible records were distinguishable. Therefore, experimental records meeting this condition were compared.

Kinetic identifiability in detection of microscopic reversibility violations. For ion channel systems that lack subconductance states (conformations with conductance intermediate between open and closed), distinguishing between equilibrium and non-equilibrium mechanisms can be difficult. Irreversible transitions may not be detected if they connect states that cannot be distinguished. However, kinetic criteria are also valid for identifying states.

A cyclic mechanism with three different bursting states (**Figure S4a**) provides an example of a mechanism that contains kinetically identifiable states. For this mechanism, the bursting states differ in their opening rate constants, and are linked by irreversible transitions. Rate constants are as follows (sec^{-1}): k_{12}, k_{23}, k_{31} = 1, k_{13}, k_{32}, k_{21} = 0.001, k_{41}, k_{52}, k_{63} = 1000, k_{14} = 100, k_{25} = 400, and k_{36} = 1600. Simulations indicate that the open probability varies in a regular, cyclic fashion; open probabilities shift from low to medium to high, and then back to low (**Figure S4b**). The third-order correlation function calculated from this record (averaged over 50 ms windows) is asymmetric (**Figure S4c**). Thus, even though this mechanism contains only two classes of conductance states (open and closed), the kinetic identifiability of states allows violations of microscopic reversibility to be observed. A similar result is observed when only two of the bursting states exhibit different open probabilities, i.e., $k_{14} = k_{25}$ = 400 sec^{-1} and k_{36} = 1600 sec^{-1}. (**Figure S5**).

In contrast, violations of microscopic reversibility are not detectable for a non-equilibrium cyclic mechanism in which the bursting states have identical kinetic properties, i.e., $k_{14} = k_{25} = k_{36}$ = 400 sec^{-1}. Simulations of this mechanism indicate that the open probability does not vary

with time (**Figure S6a**), and the third-order correlation function is symmetric (**Figure S6b**). In this case, there are not enough kinetically identifiable states for microscopic reversibility violations to be detected.

These simulations illustrate that a channel with only two conductance states may still have a sufficient number of kinetically identifiable states to detect violations of microscopic reversibility. However, a non-equilibrium process may not exhibit observable violations of microscopic reversibility due to a lack of kinetically identifiable states as shown in present simulations. As for other tests of microscopic reversibility, the absence of detectable microscopic reversibility violations thus does not rule out a non-equilibrium mechanism. Nonetheless, the detection of microscopic reversibility violations indicates that a sufficient number of kinetically identifiable states are present, and channel gating is not an equilibrium process.

References

(1) Steinberg, I. Z. *Biophysical Journal* **1986**, *50*, 171.

(2) Qian, H.; Elson, E. L. *Proc Natl Acad Sci U S A* **2004**, *101*, 2828.

Figure S1. Third-order correlation function of experimental records from K_{ATP} channels.

Numbers in the bar indicate the amplitude of third-order correlation functions.

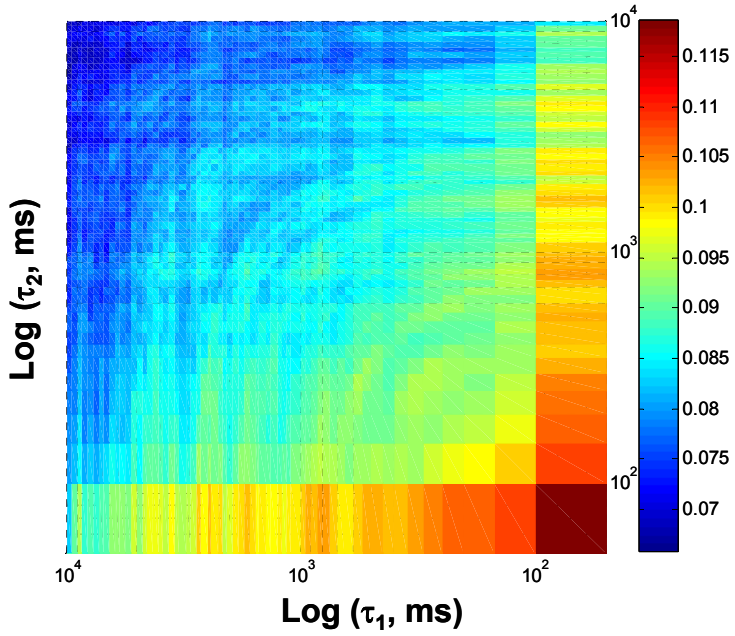

Figure S2. Cyclic mechanism for channels with bursting/non-bursting states. (a) Rate constants violating detailed balance: $k_{12} \times k_{23} \times k_{34} \times k_{41} >> k_{14} \times k_{43} \times k_{32} \times k_{21}$. (b) Rate constants satisfying detailed balance: $k_{12} \times k_{23} \times k_{34} \times k_{41} = k_{14} \times k_{43} \times k_{32} \times k_{21}$.

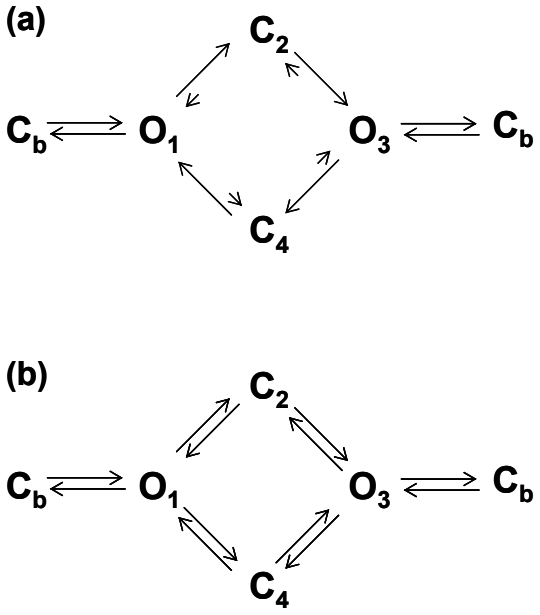

Figure S3. Third-order correlation functions from simulated records. (a) Simulated records with the violations of detailed balance show $G_2 - G_2^T$ of 0.01 ± 0.001 (N = 5, S.E.M.). (b) Simulated records for a gating reaction at equilibrium have $G_2 - G_2^T$ of 0.006 ± 0.001 (N = 5, S.E.M.).

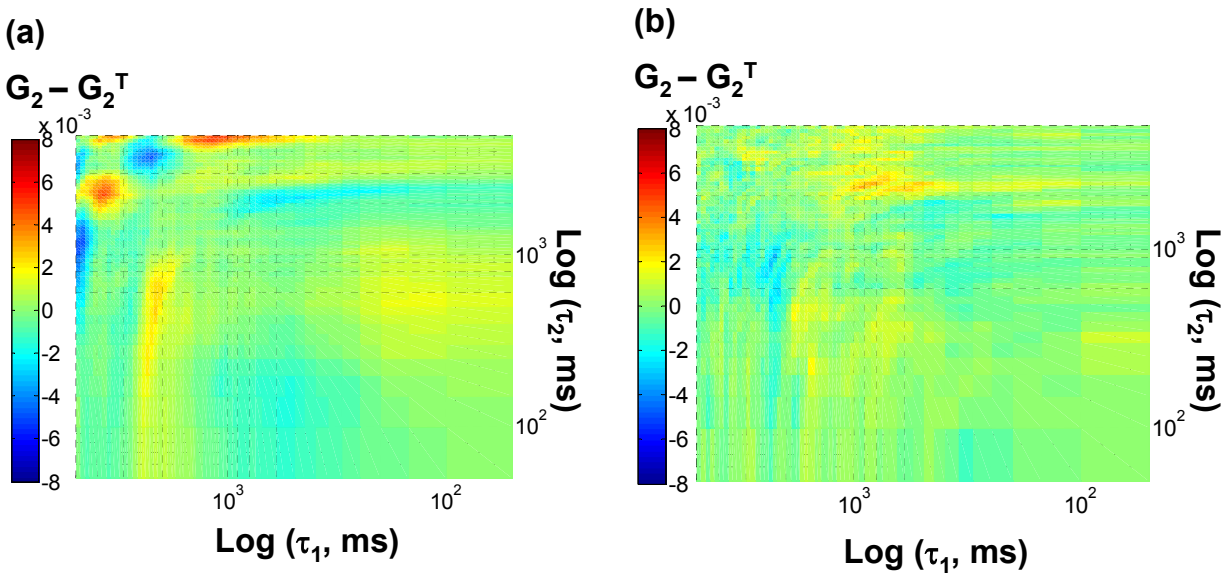

Figure S4. Kinetic identifiability in detection of microscopic reversibility violations. (a) A cyclic mechanism with three different bursting states. (b) The open probabilities shift from low to medium to high, and then back to low. (c) The third-order correlation function is asymmetric.

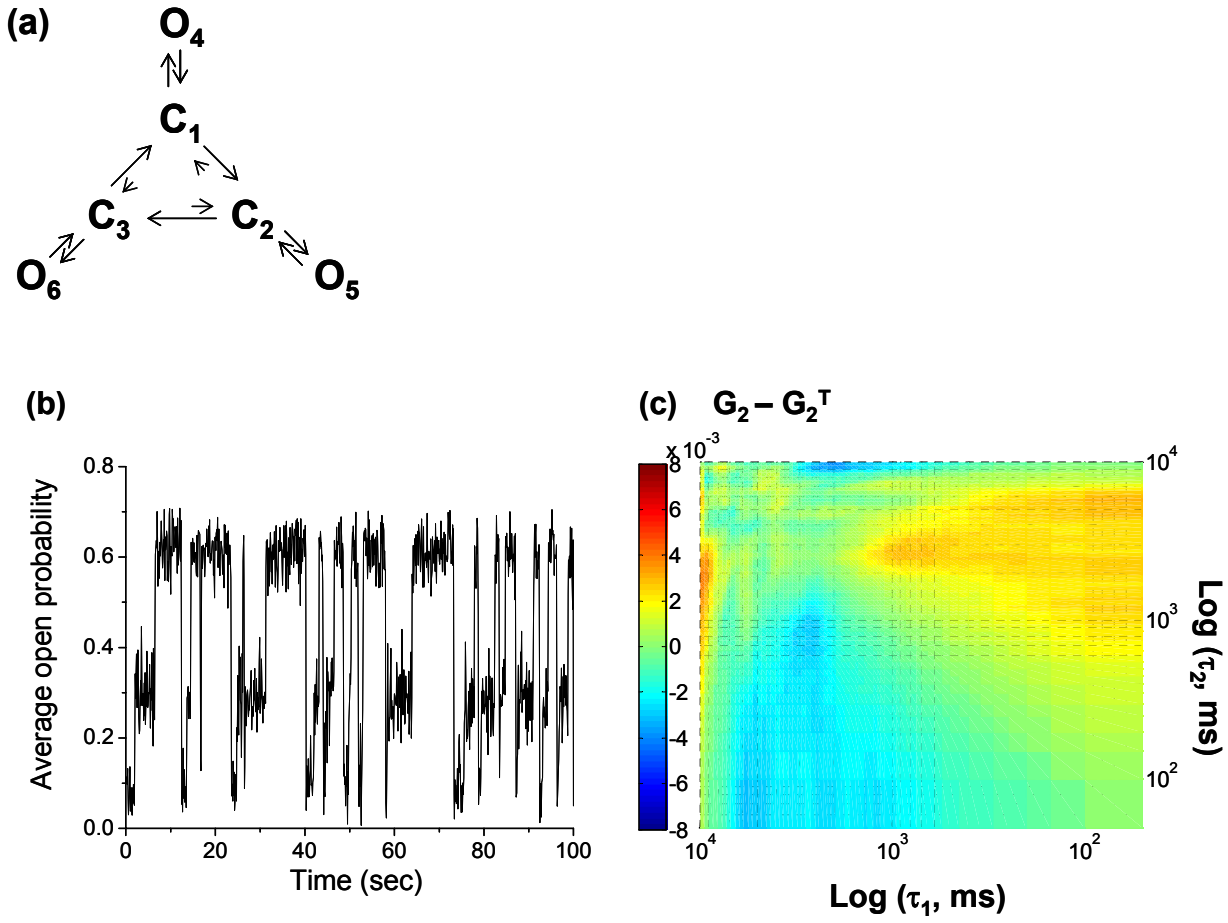

Figure S5. Only two kinetically identifiable bursting states. The asymmetric third-order correlation function is observed when only two of the bursting states exhibit different open probabilities.

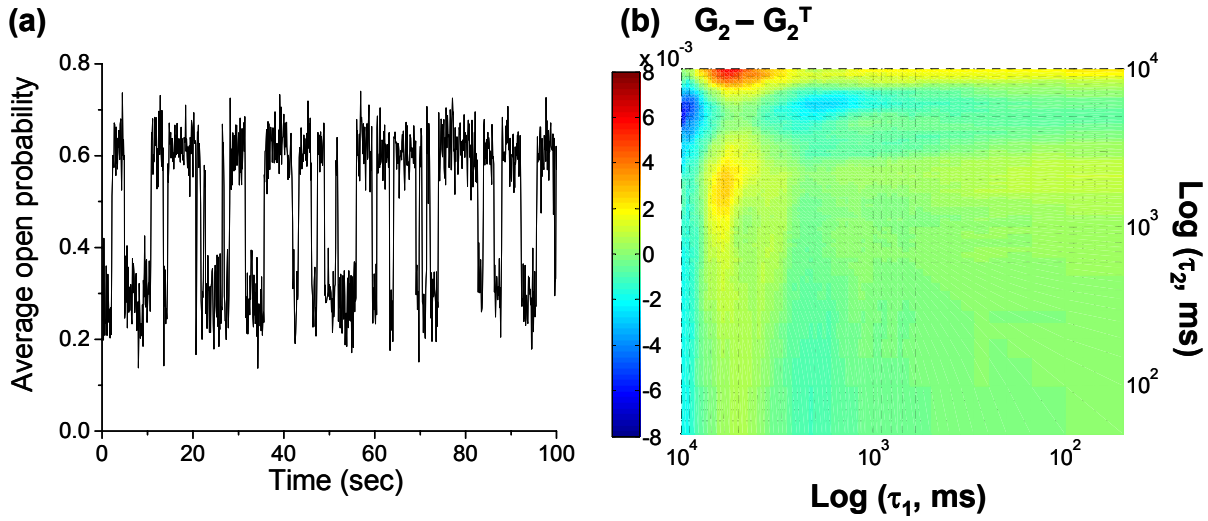

Figure S6. A kinetically non-identifiable and non-equilibrium cyclic mechanism. (a) The open probability does not vary with time. (b) The third-order correlation function is symmetric.